Радиофизика и радиоастрономия, 2009, т. 14, №1, с. 77-83

Subpixel Detection of Spectrum Images by Photodiode Structures

A. Yegorov, V. Yegorov, and S. Yegorov

O. Ya. Usikov Institute for Radiophysics and Electronics of NAS of Ukraine,
12, Akad. Proskury St., Kharkiv, 61085, Ukraine

Received April 17, 2008

The present paper is devoted to the issues of enhancing the photometer's resolving power when the spectrum images are detected by linear image sensors on emission spectrometers. Here we focus our attention on the case where the size of a photodiode structure pixel exceeds the width of the point-spread function of an optical device. It is shown that a combination of the parallel detection of all points of an image with its successive shift relative to a recording structure ensures proper recording of thus obtained image, hence the optical section of the device with an arbitrarily large sensor pixel having no loss of resolution. The problem pertaining to measurement data handling reduces to finding a solution to the inconsistent set of linear equations. An algorithm is suggested for solving the derived system of equations. The results illustrating the operation of this particular algorithm are herewith shown.

Introduction

Optical image sensors offer a certain set of parameters. In terms of the specific problem to be solved a set of parameters is likely to be variable. Specifically it includes resolution, photometric accuracy, speed of response, etc. In most cases the performance quality of imaging optical system is evaluated by its resolving power. The optical system resolution is determined by its point-spread function, which is a sort of the system's response to the δ-like effect at the input. For an optical device this effect is produced by a signal from a point source. The dimensions and shape of the point source image are largely dependent upon the diffraction phenomena at the device's aperture, optical aberrations, sensor resolution and other factors. The space resolution of image sensors is primarily determined by the dimensions of an elementary detecting cell. For the case of photographic plate, the role of an elementary cell is played by the size of the photo-emulsion grain, whereas for the linear image sensors and matrices – by a photodiode element (pixel). The typical dimensions of the photo-emulsion grain and the pixels of solid-state charge-coupled devices (CCD) are about the same order and equal to ~10 мм. Therefore a transition from photographic recording to the CCDs was not followed by a noticeable change in resolution. The fact that photo-materials used in photo- and movie cameras are being rapidly replaced by the CCDs and fall into disuse strongly suggests that these latter are convenient in service, operationally capable of being quickly readjusted, computer-compatible, and in the end they do offer lots of advantages [1, 2, 3]. By now, neither a widespread photo-emulsion nor mass-produced CCDs are capable of providing a resolution limit of light-gathering optics. The stronger the aperture ratio of the feeding optics is, the smaller is the diffraction image size of a luminous point [4]. For instance, with an instrument aperture ratio equal to 1 this size is on the order of an optical wavelength magnitude. For a visible spectrum it will be around 0.5 μm, while for the ultraviolet it will accordingly be several times smaller. The simplest way of tackling this problem is to reduce the pixel size at least by an order of magnitude, in which case a great many technological difficulties are bound to arise. Hence, some alternative methods are to be found to deal with the above problem.

1. Treatment of the Problem in a Spectral Representation

One of the ways to enhance the detector's resolving power is, e. g., optimum filtering based upon the deconvolution filter that provides for the rise in upper space frequencies. Note that the greater is the signal-to-noise ratio within the frequency range of interest, the stronger is the effect produced by this particular filter. As a result, this type of a filter cannot reconstruct those portions of the spectrum of the signal to be recorded, where the transfer function of the sensor gets nulled.

To estimate the efficiency of this type of filtering, consider the transfer function of a linear image sensor whose pixel size is equal to w. In this one-dimensional case, the module of Fourier transform can be regarded as a sensor transfer function of the sensitivity distribution along a pixel. Once the sensitivity is uniform (constant), it can be graphically shown as a rectangular pulse with perfectly steep edges. The Fourier transform module $G(k)$ of such a pulse is that of function $\sin(\pi wk)/\pi wk$ (see curve 1 in Fig. 1 on a logarithmic scale, k means relative spatial frequency).

Just for comparison, in the same figure shown is curve 2 for the Fourier transform of a flat-edge bell-shaped pulse. A Gaussian pulse was modeled by an exponential normal-distribution function with a unit amplitude and a half-width of ~0.4 w . The width is specified by normalization conditions so that an area beneath the Gaussian and rectangular pulses is the same. As evident from the comparison, the transfer function behavior for these two cases is tangibly different. The module of the sensor transfer characteristic in the high-space frequency range for curve 1 is on many orders of magnitude higher than that for curve 2. This difference gives good reason to expect that (in view of the case of curve 1), as signal-to-noise ratios are large, the sub-pixel resolution can certainly be achieved through the use of the appropriate data handling procedure. The great drawback of the relationship shown by curve 1 are the dips on some of space frequencies. This property is inherent to a sensor whose regular structure is composed of similar-in-type photodiode elements. In some instances, a photographic plate has a texture in which the size of a grain and solid-state image sensor pixel, on the average, identical. This may produce a more informative image than a photodiode structure can, which is caused by a certain spread in the size of photoemulsion grains and their random arrangement. This is more pronounced in recording one-dimensional objects, in particular, spectra [5]. In Fig. 2 curve 1 corresponds to an averaged module of the transfer function of the sensor whose pixels differ in size (a width 0.6w, 1w and 1.4 w).

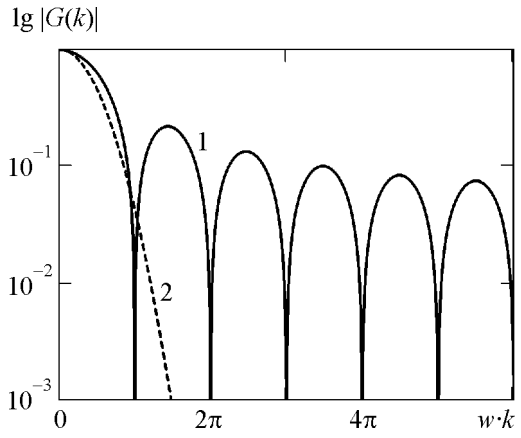

Fig. 1. *The transfer function $G(k)$ of the sensor with a rectangular (1) and bell-shaped (2) sensitivity distribution along a pixel*

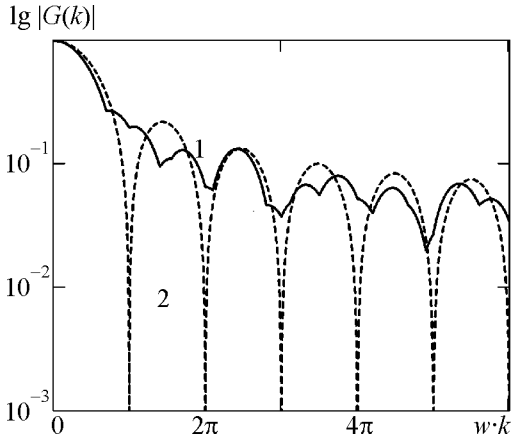

Fig. 2. *Comparative characteristics of the transfer function of the sensor whose pixels are of different (1) and similar (2) size. Scale of the axes being similar to Fig. 1*

Fig. 2 indicates that oscillations of the total transfer characteristic of this sensor are substantially attenuated as against the sensor whose pixels are of the same size with a half-width w (curve 2) smoother curve can be plotted by adding to the variety of values of pixel half-width. In practice, this type a sensor could well be made feasible by splitting a luminous flux into parallel beams and recording one and the same image with the aid of several sensors having different pixel dimensions. A similar effect can be produced by the imaging cameras of the same kind which are fitted with optical channels of different magnification. Both of these variants lead to significant sophistication of photo-detecting equipment. The hardware realization of this technique appears to be more simplified in a sequential variant, which can only be utilized for time-independent images.

Essentially, the sequential variant implies that, as an optical image is being detected by a multichannel detector, this image is shifted with respect to the image sensor pixels. This method was referred to in [6] where a description was given of using it during the photometric spectral measurements, i. e. for a one-dimensional case. A transition to a two-dimensional image does not offer any crucial distinctions.

We have also followed this particular method for the one-dimensional case when imaging emission spectra. On frequent occasions, a signal in a high-transmission emission spectrometer is considerably higher than the sensor's dark current. In this connection, a sufficient photometric accuracy is achieved through short-term single exposures on the order of 0.1 s. Yet, as a specimen under study undergoes slow heating and evaporation, the overall measurement period needs to be substantially extended, occasionally, up to several minutes. Thus, in most cases the spectral measurement time involves a set of N-single exposures. We suggest that each of the N exposures be made after the spectrum has been shifted by a $1/N$ width of a pixel. Technically, this procedure is quite feasible, e. g., by turning a plane-parallel plate mounted right behind the spectrograph slit. In this case using the spectral curve allows to get the counts-off whose number will be N times greater than that usual. The shifting of the spectrum relative to a linear image sensor just within a single pixel during successive exposures not only improves the photometric accuracy, as the measurement data are being properly handled, but also makes it possible for the spectral device to take the full advantage of its entire resolving power even if that device offers relatively wide pixels of a detecting linear image sensor. In a number of cases, this additional potential of the system may even prove to be more useful than the photometric accuracy itself.

2. Treatment of the Problem in a Coordinate Representation

In [6], we have earlier referred to, no description is given of an algorithm for solving this particular problem. In searching for an adequate algorithm we have been looking into the inherent potentialities of utilizing spectral and coordinate representation of a signal. In our specific case, the signal is an irregular sequence of peaks against the dark current and other photodetector noise. The shape of the peaks is governed by intensity distribution within a spectral line. As the spectrometer optical unit resolution increases, the above shape of the peaks tends to a δ-function. The δ-like signal has a wide spectrum that decreases with frequency. In our instance, the noise can be considered as white. Therefore the signal-to-noise ratio in a HF region tends to diminish. In order to solve a number of spectrometric problems we have employed an algorithm whose essential features can be appreciated from the following simplified examination. Let two data files (obtained while shifting a linear image sensor by a pixel half-width) be sequentially recorded. Here we have the case where $N = 2$. The whole problem is to find an array of a doubled length, which corresponds to the double resolution of the linear image sensor. The solution to this problem is found in terms of a set of linear equations like:

$$M \cdot X = B, \qquad (1)$$

where $M = \begin{pmatrix} 110.....000 \\ 011.....000 \\ ..... \\ 000.....110 \\ 000.....011 \end{pmatrix}$,

X is the sought vector, B is the measurement data vector.

In vector B the even and odd components are related to two exposures taken as the linear image sensor is shifted by a pixel half-width. If the half-width of the line is considerably smaller than that of a pixel, then it is not improbable that the resolving power might be increased many times ever rather than twice as much. In this case N is set equal to a greater number than 2 and, accordingly, a quantity of unities in the rows of matrix M tends to grow.

It should be noted that system (1) is undefined even though noises are unavailable, because the number of unknowns is always greater by one than that of equations. However, this difficulty can be overcome through the use of numerous a priori data provided by spectral measurements. This situation allows writing additional equations and find a correct solution to the system. If the half-width of a spectral line is well smaller than the pixel width, then the resolving power might as well be raised by several folds rather than by a factor of 2 only. One of the conceivable versions of a priori data can be afforded by the magnitudes of the spectral curve in the gaps between the above lines. In general an emission spectrum tends to exhibit a wavelength-dependent (λ-dependent) non-uniform distribution of spectral density (Fig. 3). This is one realization of the TMH lamp spectrum.

In between the spectral lines the curve for the wavelength-dependent luminous flux intensity for the emission spectrum is relatively flat. In this case, the entire spectrum can be broken down into the areas whose beginnings and ends lie in the domains between the spectral lines. Using the interpolation formula in these domains yields small errors for interpolated values, which can be employed as a priori data. Given the value of the function is assigned at both ends of the measuring interval we arrive at the overdetermined sets of equations whose matrices assume the following form:

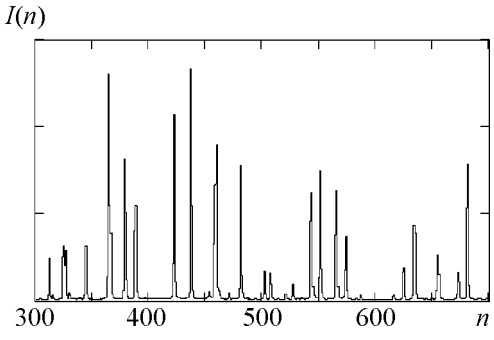

Fig. 3. *Atomic emission spectrum I(n) of gas-discharge tube, n is the number of a pixel of a recording linear image sensor*

$$M = \begin{pmatrix} 1000.....0000 \\ 1100.....0000 \\ 0110.....0000 \\ ..... \\ 0000.....0011 \\ 0000.....0001 \end{pmatrix}. \qquad (2)$$

With a redundant number of equations it would be advisable to seek an adequate solution with a least-squares procedure [7, 8]. In this case the problem is to find a solution to the following system:

$$M^T \cdot M \cdot X = M^T \cdot B, \qquad (3)$$

where the upper index T denotes the transposition of matrix M.

For the case (2) matrix $M^T \cdot M$ is written as:

$$M^T \cdot M = \begin{pmatrix} 2100....0000 \\ 1210....0000 \\ 0121....0000 \\ ..... \\ 0000....0012 \end{pmatrix}. \qquad (4)$$

For large spectrum portions the dimensionality of M runs up to several thousands. However, as this particular matrix is of co-diagonal type, the system in question is solved with no difficulties whatsoever. It is easy to make sure that the numerical value of the determinant of the square matrix (4) of size $m \times m$ always is equal to $m+1$. With the proviso that

$$b = M^T \cdot B,$$

the components of vector *b* will make the sum of two adjacent components of vector *B*:

$$b_i = B_i + B_{i+1}.$$

Using the above designations the solution of system (3) can be given as:

$$X = \frac{1}{\left|M^T \cdot M\right|} \cdot K \cdot b, \qquad (5)$$

where the matrix of coefficients *K*, which can be referred to as weighting ones, is formed using the mathematico-deductive method with no computational procedures whatsoever. As an example, for the set of equations with four unknowns we have:

$$K = \begin{pmatrix} 4 & -3 & 2 & -1 \\ -3 & 6 & -4 & 2 \\ 2 & -4 & 6 & -3 \\ -1 & 2 & -3 & 4 \end{pmatrix}.$$

As regards the sets of equations with other *m*, matrix *K* has a different dimensionality and other values of the elements. However, in spite of this the common properties they share are as follows:

1) matrix *K* regardless of its dimensionality is symmetric with respect to the diagonal;

2) the magnitude of the elements is linearly decreasing to the modulus with an increase in distance from the diagonal element;

3) along the rows and the columns there occurs an alternating sequence.

The above-mentioned common properties will suffice for generating matrix *K* of any dimensionality. This strategy allows the fast algorithm to be implemented in solving this particular problem.

Moreover, the computational difficulties over solving equation (3) are substantially reduced when splitting the spectrum interval to be reconstructed into a set of areas "jointed" by their ends. In calculating the values of the components of vector *X* from expression (5), a row of matrix *K* is multiplied by vector *b* derived from measurement data. Owing to the second property of matrix *K* a maximal contribution to value X_i is made by *i*-th and $(i \pm 1)$-th elements of the measurement data vector. The data from measuring vector B_i with indices $i \pm 2$, $i \pm 3$, ... have a slight impact upon value X_i. For the same reason the impact of the noise component vector *b* is likewise insignificant.

3. Experimental Results

The algorithm described enables one to arrive at an accurate solution in the case where the noise is nonexistent and the transfer function of the measuring system remains unchanged for two successive exposures. In the real experimental environments it is quite a challenge to provide for steady-state regimes. What is more, the noises are, in fact, apt to provide non-recurrent data. This gives rise to the oscillation of vector *X*, which is similar to the one described in [9], where different smoothing procedures for suppressing those oscillations are suggested.

We have made use of this algorithm for a two-fold definition of the spectrum image using the experimental setup comprising of the ISP-51 spectrograph and a recording system based upon the ILX511 multi-cell sensor (SONY company) whose pixel width is 14 μm. The spectrogtaph has an aperture ratio of 1:5.5. It can be used to provide an image of a glowing spot 6.6 μm in diameter the diffraction limit for a 0.5 μm light wave. This diameter is two time smaller than the pixel size of multi-cell sensor ILX511. To shift the spectrum image relative to photodetector, a plane-parallel quarz plate of ~2 mm thick was placed in between the slit and collimator of spectrograph in close proximity to the slit. This plate was rotated in the exposure latitudes with a spacing of around $4 \cdot 10^{-3}$ radian. With this plate rotation a spectrum image was displaced by an amount nearly equal to the tenth fraction of the pixel width. In this way the number of samples we had obtained on the spectrogram was on the order greater than was considered to be the case. In preprocessing an already recorded array the measured data were subjected to smoothing out and normalizing. Using the smoothed-out spectrogram

a series of averaged values was derived with a spacing strictly equal to the half of the pixel width.

Fig. 4 shows a scaled-up fragment of the spectrum shown in Fig. 3 on the interval between the 357-th and 398-th pixel.

Fig. 5 shows the same fragment with a doubled resolution as obtained by the effect of the algorithm described above.

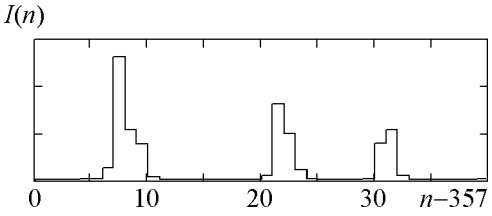

Fig. 4. *The fragment of the spectrum shown in Fig. 3 prior to its processing. Scale of the axes being similar to Fig. 3*

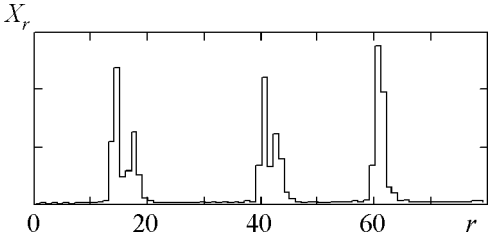

Fig. 5. *The result from processing the measurement data. X_r and r are the array and number of the processed data*

4. Conclusions

The comparison between the initial and processed graphic data illustrated in Fig. 4 and Fig. 5 is a convincing proof of the merit of our approach to the problem of subpixel resolution in spectral investigations. This allows to get rid of the interfering impact of adjacent spectral lines and obviate an adverse phase effect in photometric measurements of spectra. This particular effect was studied by the authors in [10].

Basically, the algorithm that has been scrutinized might as well be used to increase the resolution of the recording system up to the diffraction optical resolution of the device in the case of arbitrary dimensions of an image sensor pixel. If half-width of a spectral line is greater than the pixel width, then this method is found to be on a losing side in terms of getting an appropriate resolving power. The applicability scope of this technique is strongly dependent upon the behavior of the signal-to-noise ratio with an increase in the signal space frequency.

References

1. V. A. Labusov, V. I. Popov, A. V. Bekhterev, A. N. Putmakov, A. S. Pak, "Larg-size multicell solid-state radiation detectors for atomic-emission spectroscopy analysis", *Analytics and Control*, vol. 9, No. 2, pp. 104-109, 2005 (in Russian).
2. V. A. Labusov, V. I. Popov, A. N. Putmakov, A. V. Bekhterev, D. O. Seljunin, "MESA analyzers and their use as systems of recording and processing of atomic-emission spectra", *Analytics and Control*, vol. 9, No. 2, pp. 110-115, 2005 (in Russian).
3. V. A. Labusov "Multichannel optical imagery analyzers for atomic-emission spectral analysis", *Abstract of a PhD thesis: 05.11.07.*, Novosibirsk, 2005, 21 p. (in Russian).
4. M. Born and E. Wolf, *Principles of Optics*, 2nd rev. ed. New York: Pergamon Press, 1964, p. 433.
5. I. R. Shelpakova, V. G. Garanin, T. A. Chanisheva, "Analytical capabilities of a multichannel emission spectrum analyzer (MESA) for the spectral analysis", *Analytics and Control*, vol. 3, No. 1, p. 36, 1998 (in Russian).
6. E. H. van Veen, S. Bosch, "Quantitative survey analysis by using the full inductively coupled plasma emission spectra taken from a segmented charge coupled device detector: feasibility study", *Spectrochim. Acta.*, B, vol. 52, p. 323, 1997.
7. C. Lancros, *Applied Analysis.* New Jersey: Prentice Hall, Inc., 1956, p. 171.
8. Chein-I Chang, Hsuan Ren, Chein-Chi Chang, Francis D'Amico, James O. Jensen, "Estimation of Subpixel Target Size for Remotely Sensed Imagery", *IEEE Trans. Geosci. Remote Sensing*, vol. 42, No. 6, pp. 1309-1320, June 2004.
9. B. Frieden "Improvement and restoration of an image", *Collection of papers*, T. Huang, Ed. "Picture processing and digital filtering" New York: Springer-Verlang, 1975, p. 199.
10. A. D. Yegorov, V. A. Yegorov, S. A. Yegorov, E. V. Zdor, "The Photometry of Emission Optical Spectrum by Line Image Sensors", *Radiophysics and Electronics*, Kharkiv: O. Ya. Usikov Institute for Radiophysics and Electronics of NAS of Ukraine, vol. 7, No. 2, pp. 422-425, 2002 (in Russian).

Субпиксельная регистрация изображений спектров фотодиодными структурами

А. Д. Егоров, В. А. Егоров, С. А. Егоров

Работа посвящена вопросам повышения разрешающей способности фотометра при регистрации изображений спектров фотодиодными линейками на эмиссионных спектрометрах. Рассматривается случай, когда размер пиксела фотодиодной структуры превосходит размеры пятна замытия оптического прибора. Показано, что сочетание параллельного способа регистрации всех точек изображения с последовательным его смещением относительно регистрирующей структуры позволяет зарегистрировать полученное таким образом изображение без потери разрешающей способности оптической части прибора при произвольно большом пикселе детектора. Задача обработки результатов измерений сводится к решению несовместной системы линейных уравнений. Предлагается алгоритм решения полученной системы уравнений и приводятся результаты, иллюстрирующие действие этого алгоритма.

Субпіксельна реєстрация зображень спектрів фотодіодними структурами

А. Д. Єгоров, В. А. Єгоров, С. А. Єгоров

Робота присвячена питанням покращення роздільної здатності фотометра при реєстрації зображень спектрів лінійками фотодіодів на емісійних фотометрах. Розглядається випадок, коли розмір піксела фотодіодної структури перевищує розміри плями розмитості оптичного приладу. Показано, що поєднання паралельного способу реєстрації усіх точок зображення з його послідовним зміщенням відносно фотодіодної структури дозволяє зареєструвати одержане таким чином зображення без втрати роздільної здатності оптичної частини приладу за довільно великого піксела детектора. Задача обробки результатів вимірювання зводиться до розв'язання несумісної системи лінійних рівнянь. Пропонується алгоритм розв'язання одержаної системи рівнянь та наводяться результати, що ілюструють дію цього алгоритму.